10B.6 INTERANNUAL TELECONNECTION BETWEEN URAL-SIBERIAN BLOCKING AND THE EAST ASIAN WINTER MONSOON

HO NAM CHEUNG[1,2] AND WEN ZHOU[1,2*]
[1]City University of Hong Kong Shenzhen Research Institute
[2]Guy Carpenter Asia-Pacific Climate Impact Centre,
School of Energy and Environment, City University of Hong Kong

1. INTRODUCTION

Blocking describes a large-scale extratropical anticyclone to remain quasi-stationary longer than synoptic time scales, which potentially triggers various climate extremes across its upstream and downstream. Its recurrence over Ural-Siberia during winter persistently reinforces the Siberian high such that a long-lasting cold period may result in East Asia, such as February-March 2005 (Lu and Chang 2009) and January 2008 (Zhou *et al.* 2009). In the past few decades, however, the blocking activities over this region underwent a remarkable declining trend that may be responsible for a warmer East Asian winter climate (L. Wang *et al.* 2010). These motivate us to better understand the linkage between Ural-Siberian blocking (USB) and the East Asian winter monsoon (EAWM).

The EAWM activities activate the interaction between mid-latitude and tropical regions (Lau and Li 1984; Chang *et al.* 2006). They are affected by the climate factors on both sides. On one hand, Gong *et al.* (2001) identified a negative correlation between the Siberian high intensity and the Arctic Oscillation (AO). This relationship may be explained by an eastward-propagating wavetrain signal across Eurasia (Joung and Hitchman 1982; Takaya and Nakamura 2005). During the negative phase of AO, such a wavetrain is likely to undergo stronger manifestation and contributes to stronger regional cold air activities associated with USB, and vice versa (Park *et al.* 2011).

On the other hand, the EAWM tends to be stronger (weaker) in La Niña (El Niño) years. This is due in part to the northwestward propagation of an anomalous cyclonic (anticyclonic) flow over the Philippines, which is associated with the sea surface temperature anomalies of ENSO (Chen *et al.* 2000; Wang *et al.* 2000). Wu and Leung (2009) suggested that warmer winters in El Niño years may also be accompanied by fewer occurrences of USB. Therefore, the impacts of the AO and ENSO on the EAWM may be related to USB activities.

This study attempts to study the blocking-EAWM relationship by considering the combined effect of the AO and ENSO. Data and methods are presented in section 2. Section 3 describes the two major USB patterns. Afterward, section 4 analyzes the combined effect of the AO and ENSO. The results are summarized in Section 5.

* *Corresponding author:* Dr. Wen Zhou, City University of Hong Kong Shenzhen Research Institute, Guy Carpenter Asia-Pacific Climate Impact Centre, School of Energy and Environment, City University of Hong Kong; e-mail: wenzhou@cityu.edu.hk

2. DATA AND METHODS

2.1 Data and study period

The study period includes the five consecutive months from November to March (NDJFM) for the period 1950/51 to 2009/10. Raw data were extracted from NCEP-NCAR reanalysis datasets (Kalnay *et al.* 1996).

2.2 Detection of blocking and study region

The blocking event detection algorithm generally follows that introduced by Barriopedro *et al.* (2006). It begins with identifying the blocking longitudes at each longitude grid point (λ), which are determined by the meridional gradients of 500-hPa geopotential height (Z500) over the extratropical region (ZGN and ZGS). A longitude is said to be blocked when one of the five latitude pairs (ϕ_N, ϕ_0, ϕ_S) fulfilling the two equations. A blocking region has to be made up of at least 5 neighbouring blocking longitudes.

$$\mathrm{ZGN}(\lambda) = \frac{\mathrm{Z500}(\lambda,\phi_N)-\mathrm{Z500}(\lambda,\phi_0)}{\phi_N-\phi_0} < -10m/\deg\mathrm{lat}$$

$$\mathrm{ZGS}(\lambda) = \frac{\mathrm{Z500}(\lambda,\phi_0)-\mathrm{Z500}(\lambda,\phi_S)}{\phi_0-\phi_S} > 0$$

where $\lambda = (0, 357.5)^{o}$E, $\phi_N = 80^{o}$N + Δ, $\phi_0 = 60^{o}$N + Δ, $\phi_S = 40^{o}$N + Δ, and $\Delta = -5^{o}$, -2.5^{o}, 0^{o}, 2.5^{o} and 5^{o}.

Figure 1 shows that the blocking frequency over Ural-Siberia in January 2008 surpasses the 95-th percentile for the period 1950 and 2007. In this study, the area of interest of blocking is narrowed to 30°-100°E.

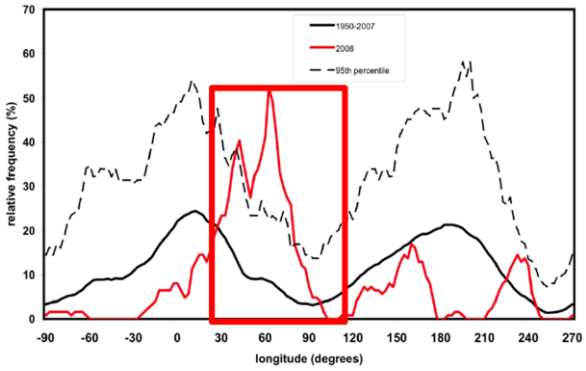

FIGURE 1. The climatology (black solid) and 95-th percentile (black dashed) of blocking frequency over the Northern Hemisphere in January during 1950-2007. The blocking frequency in January 2008 is indicated by the red solid line (From Zhou *et al.* 2009). The red box encloses the area of interest in this study.

2.3 East Asian winter monsoon indices

Due to distinct modes of the EAWM (Wu *et al.* 2006), there is no unique index able to capture its interannual variability. We use three EAWM indices, including the Siberian high intensity (SHI; sea level pressure over 40°-65°N, 80°-120°E; Panagiotopoulos *et al.* 2005) and the two temperature modes introduced by B. Wang *et al.* (2010). The two temperature modes are taken as the first two eigenvectors of 2-m air temperature over 0°-60°N, 100°-140°E, which are called TM1 and TM2 hereafter (Figure 2).

The TM1 (TM2) mode has a center of action in the northern (southern) part of the domain. Moreover, it is noticeable that the signs over the north and the south of the (TM1) TM2 mode are the same (opposite). For convenience, the sign of the TM2 mode is reversed such that the positive sign of the TM1 (TM2) mode represents higher temperature in the north (south).

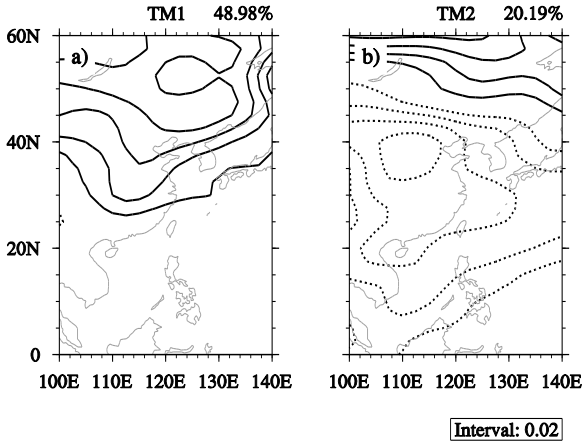

FIGURE 2. The first two eigenvectors (EOF1-2) of winter-mean 2-m air temperature in the EAWM with the explained variance shown at the top right hand side.

3. URAL-SIBERIAN BLOCKING PATTERNS

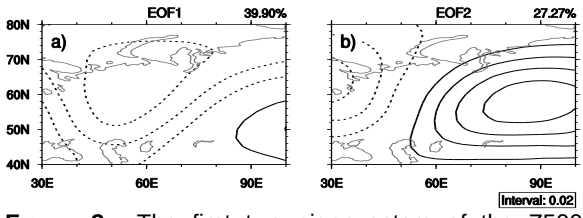

FIGURE 3. The first two eigenvectors of the Z500 (EOF1-2) over Ural-Siberia with the explained variance shown at the top right hand side.

Applying an Empirical Orthogonal Function (EOF) analysis for NDJFM-mean Z500 enclosing a domain 40°-80°N, 30°-100°E, ten EOF modes (EOF1-10) are extracted. We identify two well-separated modes that account for 67.2% of the total variance, as shown in Figure 3. Both the two dominant modes consist of a dipole pattern. The first mode is a northwest-southeast oriented dipole, which might infer the baroclicity over East Asia. On the other hand, the second mode is an east-west oriented dipole and it may represent an east-west shift of the center of action over our domain.

By considering one mode stands out in each year, 44 out of 60 years are found to demonstrate dominance in these two modes (not shown). Figure 4 shows that the blocking frequency is significantly different over the Ural Mountains (Scandinavia) under predominant EOF1 (EOF2) mode, which is higher (lower) in the negative (positive) polarity. Accordingly, the stronger (weaker) cold advection downstream of the blocking center strengthens (weakens) the cold air intensity (Figure 5).

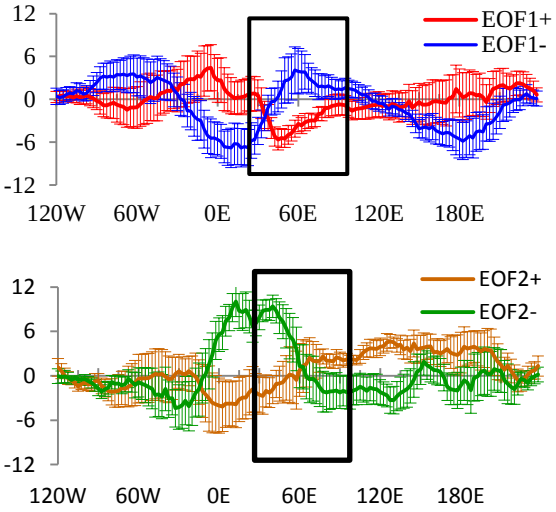

FIGURE 4. Blocking frequency anomalies over the Northern Hemisphere (days) in the years showing dominance of the EOF1 mode (upper panel) and the EOF2 mode (lower panel).

As a result of the difference in the center of action of the two EOF modes, the EOF1 mode is accompanied by uniform cooling/warming in the EAWM while the EOF2 mode gives rise to an opposite temperature anomaly pattern in East Asia. These can be described by the correlations between PC1/PC2 and the EAWM indices listed in Table 1. These results suggest two different blocking-EAWM relationships.

TABLE 1. Linear correlations between the two EOF modes and the EAWM indices, where the bold (italic) values exceed the 99% (95%) confidence level.

	SHI	TM1	TM2
PC1	**-0.653**	**0.683**	-0.094
PC2	0.214	*0.296*	**-0.449**

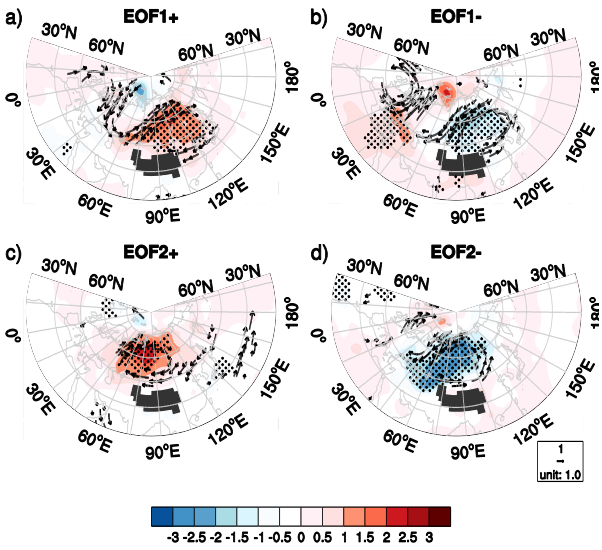

FIGURE 5. Surface air temperature anomaly (shading; unit: ^{o}C) and 500-hPa wind anomaly (vector; unit: ms^{-1}) in the winters demonstrating dominance in (a) positive EOF1 mode, (b) negative EOF1 mode, (c) positive EOF2 mode and (d) negative EOF2 mode. The air temperature enclosed by the dotted regions and the vector wind are significantly different from the 60-year climatology of air temperature and either zonal wind or meridional wind component respectively at the 95% confidence level. The Tibetan Plateau is dark shaded.

4. COMBINED EFFECT OF AO AND ENSO

The two major EOF modes resemble an eastward propagating wavetrain signal coming from the North Atlantic Ocean (not shown), so they can be depicted by the "North Atlantic-Ural-East Asia" teleconnection pattern which is related to the North Atlantic Oscillation (NAO) (Li *et al.* 2008). In this study, the AO is considered instead since it is more representative of the extratropical climate yet retains the characters of the NAO (Thompson and Wallace 1998).

On the other hand, as mentioned in the introduction, the EAWM is also affected by the tropical climate factors like ENSO. Indeed, the EAWM-ENSO relationship has been studied extensively (e.g. Li 1990; Chan and Li 2004; Zhou *et al.* 2007).

We first consider the impacts of each of the two factors on both USB patterns and the EAWM. Their correlations are summarized in Table 2.

TABLE 2. Linear correlations between the AO/ENSO and the two EOF modes and EAWM indices, where the bold (italic) values exceed the 99% (95%) confidence level.

	ENSO	PC1	PC2	SHI	TM1	TM2
AO	-0.110	**0.438**	*0.288*	**-0.336**	**0.598**	-0.183
ENSO		-0.125	-0.116	-0.115	0.008	*0.328*

4.1 *The impacts of AO*

Table 2 suggests that the impacts of the AO are analogous to those of the EOF1 mode with a center of action near the Ural Mountains (~60^{o}E). This can be illustrated by the significant difference in blocking frequency anomalies near 60^{o}E between the two polarities of the AO, as shown in Figure 6.

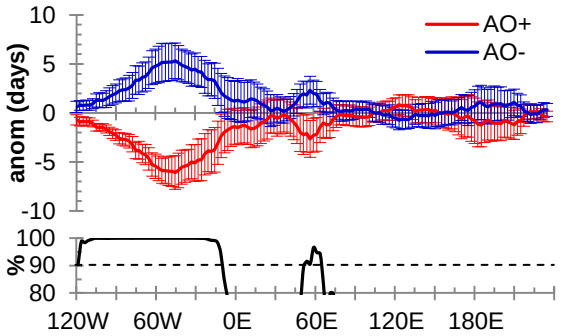

FIGURE 6. Longitudinal distribution of blocking frequency anomalies in the Northern Hemisphere under the positive phase of the AO (red) and the negative phase of the AO (blue), where the error bar represents the σ deviation (unit: days) (upper panel); Confidence level (%) for the difference in blocking frequency between the two polarities of the AO in the Student's *t*-test (lower panel).

4.2 *The modulations of ENSO*

Furthermore, Table 2 suggests that the ENSO shows a substantial linkage only with the TM2. It appears that the correlations between the ENSO and any factors with the center of action over the extratropics are very weak. Indeed, the impacts of the ENSO on USB and the EAWM are evidenced by the tendencies of the PC1 (Figure 7) and the SHI (not shown). During warm ENSO events (where the anomaly of the ENSO index is greater than 1.0^{o}C), the PC1 tends to be positive and the SHI tends to be negative. These results agree with previous findings that the EAWM tends to be weak in warm ENSO years (e.g., Li 1990; Chen *et al.* 2000). In comparison, there is no obvious tendency of either the PC1 or the SHI in cold ENSO events.

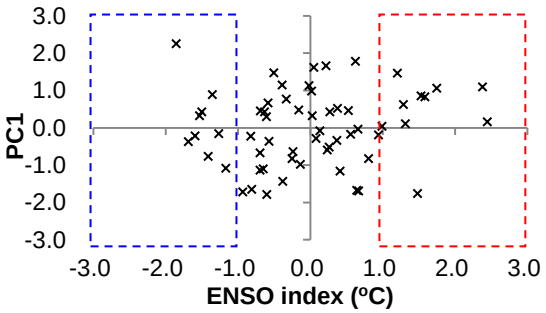

FIGURE 7. Scatter plot between the ENSO index and standardized values of the PC1, where the ENSO indices greater than 1.0^{o}C (smaller than -1.0^{o}C) are enclosed by the black (gray) dashed line.

The modulation can also be indicated by the difference in blocking frequency anomalies between the two ENSO groups. As shown in Figure 8, their differences exceed the 90% confidence level between 65° and 152.5°E. However, the frequencies in the entire region are slightly above normal in cold years in contrast to a remarkable decrease in warm years. Therefore, it is suggested that the extratropical circulation over East Asia is more sensitive to the AO. It may be modulated by the ENSO if the ENSO signal is strong enough to induce an anomalous circulation over the Western North Pacific to propagate toward East Asia. Comparatively, warm ENSO events are stronger than cold events such that their impacts on both blocking and the EAWM are more pronounced.

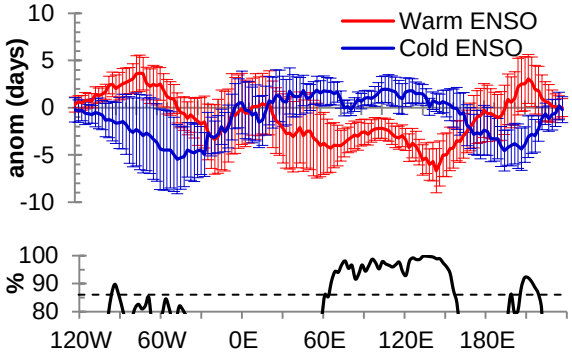

FIGURE 8. Longitudinal distribution of blocking frequency anomalies in the Northern Hemisphere during warm ENSO winters (red) and cold ENSO winters (blue), where the error bars indicate the σ deviation (upper panel); (b) Confidence level (%) for the difference in blocking frequency between the two polarities of the ENSO in the Student's *t*-test (lower panel).

4.3 Combined effect of AO and ENSO

Both the AO and ENSO exert impacts on both USB and the EAWM. Since the two climate factors are weakly correlated (Table 2), it is aware the impacts of their combined effect for which they are in phase and out of phase.

The major USB pattern is determined by comparing the magnitude of the first two leading EOFs listed in Table 3. It is suggested that the EOF1 (EOF2) mode tends to stand out for the in-phase (out-of-phase) condition. Therefore, the in-phase and out-of-phase conditions are accompanied by different blocking–EAWM relationships, as revealed in section 3.

TABLE 3. Mean and standard error of the standardized values of the first two leading principal components under different combinations of the AO and ENSO.

Combined effect		PC1	PC2
In phase	AO+ ENSO+	0.34±0.16	0.11±0.25
	AO- ENSO-	-0.45±0.23	0.08±0.23
Out of phase	AO+ ENSO-	0.24±0.28	0.28±0.27
	AO- ENSO+	-0.02±0.27	-0.41±0.23

More evidence concerning the combined effect of the AO and ENSO can be deduced by the correlation analyses listed in Tables 4–5.

When the AO and ENSO are of the same polarity, both are closely related to the PC1, the SHI, and the TM1 but are weakly correlated with the PC2 and the TM2 (Table 4). These relationships are comparable to those with only the AO given by Table 2. Since the correlation coefficient between each of these factors and the AO is of the same sign as that with the ENSO, it is suggested that the ENSO collaborates with the AO in constructing the USB–EAWM relationship.

When the AO and ENSO are of opposite polarity, on the other hand, both of them show significant correlations with the PC2 and both the TM1 and the TM2 (Table 5). However, the correlation between each of these factors and the AO is opposite in sign to that with the ENSO. This may indicate that the AO and ENSO exert an incoherent forcing on the extratropical–tropical interaction over the East Asian continent. Hence, this may explain why the two climate factors form a weak linkage with the SHI. In short, the USB–EAWM relationship is stronger (weaker) under the in-phase (out-of-phase) condition.

TABLE 4. Linear correlations between the AO/ENSO and the two leading EOF modes and EAWM indices when the AO and ENSO are in phase, where the bold, italic, and underlined values exceed the 99%, 95%, and 90% confidence levels, respectively. Note that the EOF1 is the dominant blocking pattern.

	PC1	PC2	SHI	TM1	TM2
AO	**0.524**	0.106	*-0.400*	**0.536**	0.056
ENSO	*0.394*	0.190	*-0.421*	**0.527**	0.261
PC1			**-0.665**	**0.644**	-0.180
PC2			0.199	0.234	*-0.444*

TABLE 5. Same as Table 4, but for the cases when the AO and ENSO are out of phase. Note that the EOF2 is the dominant blocking pattern.

	PC1	PC2	SHI	TM1	TM2
AO	*0.380*	*0.449*	-0.287	**0.657**	*-0.411*
ENSO	-0.065	-0.338	0.192	-0.334	*0.377*
PC1			**-0.642**	**0.743**	-0.049
PC2			0.259	0.301	*-0.437*

5. SUMMARY

An overview of the relationship between USB and the EAWM has been introduced. The spatial feature of USB is acquired by performing the EOF analysis on the winter-mean Z500. The EOF1 (EOF2) mode represents the recurrence of blocking highs over the Ural Mountains (Scandinavia), which shows a stronger (weaker) linkage with the SHI and TM1 and a weaker (stronger) linkage with the TM2. Concerning the combined effect of the AO and ENSO, the EOF1 (EOF2) mode dominates and the USB–EAWM relationship is stronger (weaker) when the two factors are in phase (out of phase), which is summarized in Figure 9.

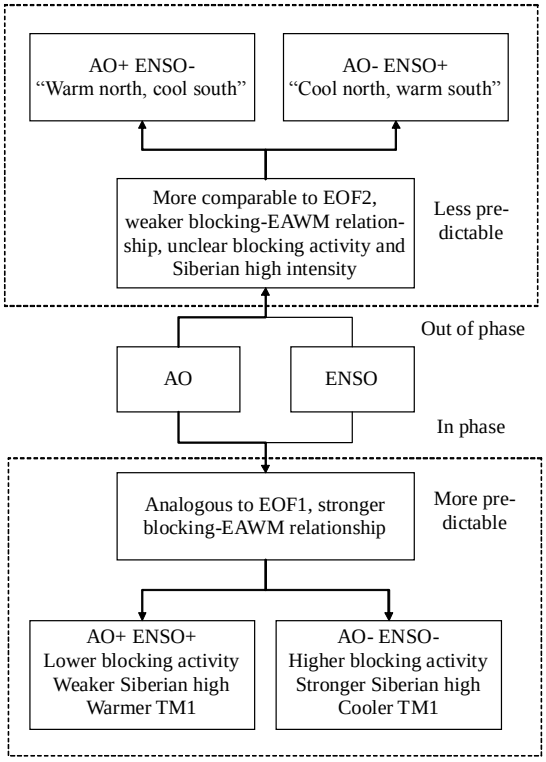

FIGURE 9. A schematic diagram for the predictability of Ural–Siberian blocking and the EAWM taking the role of the AO and ENSO into consideration.

Since the AO may undergo sharp intraseasonal transitions due to tropospheric-stratospheric interaction (Baldwin and Dunkerton 1999), further work is needed to verify the blocking–EAWM relationship at subseasonal timescales. In fact, the downward-propagating signal from the stratosphere is probably an important precursor for cold surges in East Asia (Jeong *et al.* 2006; Wang and Chen 2010). Apart from the AO and ENSO, other factors such as the snow cover over Eurasia and the sea surface temperature over the North Atlantic Ocean and Indian Ocean are also important for the prediction of the EAWM (B. Wang *et al.* 2010); these might also be considered in our future work.

Acknowledgments: More details about this study can be found in Cheung *et al.* (2012).This research is support by the Research Grants Council of the Universities Committee of Hong Kong Grant 9041548.

6. REFERENCES

Baldwin, M. P., and T. J. Dunkerton, 1999: Propagation of the Arctic Oscillation from the stratosphere to the troposphere. *J. Geophys. Res.*, **104**, 30937–30946.

Barriopedro, D., R. Garcia-Herrera, A.R. Lupo, and E. Hernandez, 2006: A climatology of Northern Hemisphere blocking. *J. Climate*, **19**, 1042–1063.

Chan, J. C. L., and C. Li, 2004: The East Asian winter monsoon. *East Asian Monsoon*, C.-P. Chang, Ed., World Scientific Series on Meteorology of East Asia, Vol. 2, World Scientific Publishing Co., 54–106.

Chang, C.-P., Z. Wang., and H. Hendon, 2006: The Asian winter monsoon. *The Asian Monsoon*, B. Wang (Ed.), Springer, Heidelberg, 89–128.

Chen, W., H.-F. Graf, and R. Huang, 2000: The interannual variability of East Asian winter monsoon and its relation to the summer monsoon. *Adv. Atmos. Sci.*, **17,** 48–60.

Cheung, H. N., W. Zhou, H. Y. Mok, and M. C. Wu, 2012: Relationship between Ural–Siberian Blocking and the East Asian Winter Monsoon in Relation to the Arctic Oscillation and the El Niño-Southern Oscillation. *J. Climate*, in press.

Gong, D., S. Wang, and J. Zhu, 2001: East Asian winter monsoon and Arctic Oscillation. *Geophys. Res. Lett.*, **28**, 2073–2076, doi:10.1029/2000GL012311.

Jeong, J.-H., B.-M. Kim, C.-H. Ho, D. Chen, and G.-H. Li, 2006: Stratospheric origin of cold surge occurrence in East Asia. *Geophys. Res. Lett.*, **33**, L14710, doi: 10.1029/2006GL026607.

Joung, C.-H., and M. H. Hitchman, 1982: On the role of successive downstream development in East Asian polar air outbreaks. *Mon. Wea. Rev.*, **110**, 1224–1237.

Kalnay, E., and Coauthors, 1996: The NCEP/NCAR 40-year reanalysis project. *Bull. Amer. Meteor. Soc.*, **77**, 437–471.

Lau, K. M., and M. T. Li, 1984: The monsoon of East Asia and its global associations—A survey. *Bull. Amer. Meteor. Soc.*, **65**, 114–125.

Li, C., 1990: Interaction between anomalous winter monsoon in East Asia and El Niño events. *Adv. Atmos. Sci.*, **7**, 36–46.

Li. J., R. Yu, and T. Zhou, 2008: Teleconnection between NAO and climate downstream of the Tibetan Plateau. *J. Climate*, **21**, 4680–4689.

Lu, M.-M., and C.-P. Chang, 2009: Unusual late-season cold surges during the 2005 Asian winter monsoon: Roles of Atlantic blocking and the central Asian anticyclone. *J. Climate*, **22**, 5205–5217.

Panagiotopoulos, F., M. Shahgedanova, A. Hannachi, and D. B. Stephenson, 2005: Observed trends and teleconnections of the Siberian high: A recently declining center of action. *J. Climate*, **18**, 1411–1422.

Park, T.-W., C.-H. Ho, and S. Yang, 2011: Relationship between the Arctic Oscillation and cold surges over East Asia. *J. Climate*, **24**, 68–83.

Takaya, K., and H. Nakamura, 2005b: Geographical dependence of upper-level blocking formation associated with intraseasonal amplification of the Siberian high. *J. Atmos. Sci.*, **62**, 4441–4449.

Thompson, D. W. J., and J. M. Wallace, 1998: The Arctic Oscillation signature in the wintertime geopotential height and temperature fields. *Geophys. Res. Lett.*, **25**, 1297–1300, doi:10.1029/98GL00950.

Wang, B., R. Wu, and X. Fu, 2000: Pacific-East Asia teleconnection: How does ENSO affect East Asian climate? *J. Climate*, **13**, 1517–1536.

———, Z. Wu, C.-P Chang, J. Liu, J. Li, and T. Zhou, 2010: Another look at interannual-to-interdecadal variations of the East Asian winter monsoon: The northern and southern temperature modes. *J. Climate*, **23**, 1495–1512.

Wang, L., and W. Chen, 2010: Downward Arctic Oscillation signal associated with moderate weak stratospheric polar vortex and the cold December 2009. *Geophys. Res. Lett.*, **37**, L09707, doi:10.1029/2010GL042659.

———, W. Chen, W. Zhou., J. C. L. Chan, D. Barriopedro, and R. Huang, 2010: Effect of the climate shift around mid 1970s on the relationship between wintertime Ural blocking circulation and East Asian climate. *Int. J. Climatol*, **30**, 135–158, doi:10.1002/joc.1876.

Wu, B., R. Zhang, R. D'Arrigo, 2006: Distinct modes of the East Asian winter monsoon. *Mon. Wea. Rev.*, **134**, 2165–2178.

Wu, M. C., and W. H. Leung, 2009: Effect of ENSO on the Hong Kong winter season. *Atmos. Sci. Lett.*, **10**, 94–101.

Zhou W., X. Wang, T. Zhou, C. Li, and J. C. L. Chan, 2007: Interdecadal variability of the relationship between the East Asian winter monsoon and ENSO. *Meteorol. Atmos. Phys.*, doi:10.1007/s00703-007-0263-6.

———, J. C. L. Chan, W. Chen, J. Ling, J. G. Pinto, and Y. Shao, 2009: Synoptic-scale controls of persistent low temperature and icy weather over southern China in January 2008. *Mon. Wea. Rev.*, **137**, 3978–3991.